Response of Non-local and Heat Source in Moore-Gibson-Thompson Theory of Thermoelasticity with Hyperbolic Two Temperature

RAJNEESH KUMAR[1], SACHIN KAUSHAL[2], GULSHAN SHARMA[2,3]
[1]Department of Mathematics, Kurukshetra University,
Kurukshetra-136119 Haryana,
INDIA

[2]Department of Mathematics, School of Chemical Engineering and Physical Sciences,
Lovely Professional University,
144411 Phagwara,
INDIA

[3]PostGraduate Department of Mathematics,
Doaba College Jalandhar,
INDIA

Abstract: - A new mathematical model of the Moore–Gibson–Thompson (MGT) theory of thermoelasticity under non-local and hyperbolic two-temperature (HTT) has been developed. The preliminary equations are put in two-dimensional form and are converted into dimensionless form. The obtained equations are simplified by applying potential functions. The Laplace transform w.r.t time variable and Fourier transforms w.r.t space variable are employed in the resulting equations. The assumed model has been used to explore the outcome of heat source in the form of a laser pulse decaying with time and moving with constant velocity in one direction. The problem is further examined with normal distributed force and ramp type thermal source. In the transformed domain, the physical field quantities like displacements, stresses, conductive temperature, and thermodynamic temperature are obtained. The resulting expressions are obtained numerically with the numerical inversion technique of the transforms. In simulation, various impacts such as non-local, heat source velocity-time, and HTT are examined and presented in the form of figures. Unique results are also deduced.

Key-Words: - Moore–Gibson–Thompson (MGT), hyperbolic two temperature (HTT), non-local, moving heat source, thermoelasticity, ramp type thermal source, normal distributed force.

Received: June 9, 2023. Revised: November 11, 2023. Accepted: December 21, 2023. Published: December 31, 2023.

1 Introduction

The theory of thermoelasticity has received intensive development from researchers due to its wide applications in the fields of architecture, structural analysis, geophysics, aeronautics, etc. The first two popular generalized theories of thermoelasticity are suggested by [1], [2], respectively. Later on [3], [4], [5], [6], proposed three different theories of generalized thermoelasticity, which are commonly known as GN-I, GN-II, and GN-III theories of thermoelasticity. However, the results corresponding to the GN-III model showed that this theory leads to a defect similar to the traditional Fourier law and predicts the instantaneous propagation of thermal waves.

Two-temperature theory of thermoelasticity was developed by [7], [8]. [9], introduced a theory of two-temperature generalized thermoelasticity. This theory has a drawback in that thermal waves were propagating at infinite speed. To overcome this obstacle, [10], modified the two-temperature generalized theory and furnished the HTT generalized thermoelasticity theory. [11], investigated the thermoelastic interactions in an infinite elastic medium with a cylindrical cavity in the context of the hyperbolic two-temperature generalized thermoelasticity theory. [12], obtained the analytical

solution by taking into account the photo-thermoelastic model under the new hyperbolic two-temperature thermoelasticity.

Recently, interest in non-local elasticity has been growing rapidly. Consideration of non-local factors, in heat conduction theory, augments the microscopic effects at a macroscopic level. It has been successfully applied to the problems of dislocation, fracture, mechanics, and dispersion of waves, [13], [14], developed the concept of the non-local theory of thermoelasticity. [15], discussed the wave propagation in a nonlocal thermoelastic medium for Green and Naghdi theory II (without energy dissipation) of generalized thermoelasticity. [16], investigated the impact of a moving heat source on a magneto-thermoelastic rod in the context of Eringen's nonlocal theory under three-phase lag with a memory-dependent derivative. [17], investigated the impacts of the nonlocal thermoelastic parameters in the Green and Naghdi model without energy dissipation for a nanoscale material by the eigen value approach.

The Moore-Gibson-Thompson (MGT) equation has attracted the serious attention of several researchers. This equation arises in many fields, such as fluid mechanics, nanostructures, and thermoelasticity. [18], has established a novel thermoelastic model subjected to Moore-Gibson-Thompson's (MGT) equation which originated from a third-order differential equation. By incorporating a relaxation time parameter into the heat equation of Green-Naghdi theory of type III. The considered model was used to analyze the well-posedness and the stability of solutions for one dimension and three-dimension problem. Later, [19], presented a generalized thermoelastic model using the MGT heat conduction equation in the context of two temperatures and proved the well-posedness and the exponential decay of the solutions.

[20], employed a modified MGT thermoelastic heat transfer model to investigate the impact of a magnetic field on isotropic perfectly conducting half-space subjected to a periodic heat source. [21], established a domain of influence theorem in the MGT thermoelasticity for dipolar bodies and analyzed wave propagation in an isotropic and infinite body subjected to a continuous thermal line source. [22], established results for the domain of influence theorem for potential–temperature disturbance in the context of MGT theory of thermoelasticity. Many authors discussed different problems in the context of MGT theory of thermoelasticity, notable of them are [23], [24], [25], [26].

The present investigation has been performed by adopting MGT theory of thermoelasticity along with non-local and HTT models. The problem is examined under heat source in the form of laser pulse decaying with time and moving with constant velocity in one direction along with normal distributed force and ramp type thermal source. After simplifying the equation with aid of dimensionless parameters, the potential functions, and integral transform techniques, the impact of non-local, HTT, and heat source velocity for normal distributed force and thermal source are examined on physical quantities and are represented in the form of graphs.

2 Basic Equations

Following [10], [13], [18], the field equations and constitutive relations in the context of MGT theory with hyperbolic two temperature in the absence of body forces can be written as:

$$(\lambda+\mu)\nabla(\nabla\cdot\vec{u})+\mu\nabla^2\vec{u}-\beta_1\nabla T=\rho\left(1-{\xi_1}^2\nabla^2\right)\frac{\partial^2\vec{u}}{\partial t^2}, \quad (1)$$

$$\left(1+\tau_0\frac{\partial}{\partial t}\right)\left[\rho C_e\ddot{T}+\beta_1 T_0\ddot{e}-\dot{Q}\right]=K^*\nabla^2\dot{\phi}+K_1\nabla^2\phi, \quad (2)$$

$$t_{ij}=\lambda u_{k,k}\delta_{ij}+\mu\left(u_{i,j}+u_{j,i}\right)-\beta_1 T\delta_{ij}, \quad (3)$$

$$\boldsymbol{T}=\left(\mathbf{1}-\boldsymbol{a}\boldsymbol{\nabla^2}\right)\boldsymbol{\phi}, \quad (4)$$

$$\ddot{\boldsymbol{\phi}}-\ddot{\boldsymbol{T}}=\boldsymbol{\beta^*}\boldsymbol{\nabla^2}\boldsymbol{\phi}, \quad (5)$$

where

λ,μ - Lame's constants, $\vec{u}$ - displacement vector, $\beta_1=(3\lambda+2\mu)\alpha_t$, α_t - coefficient of linear thermal expansion, ξ_1 - non-local parameter, t_{ij}- components of stress tensor, t-time, ρ, C_e- density and specific heat respectively, Q -heat source, K^* - thermal conductivity, $K_1=\frac{\lambda+2\mu}{4}C_e$- material constant, ∇^2 - Laplacian operator, ϕ - conductive temperature, T - thermodynamic temperature, a - two temperature parameter, τ_0- relaxation time, δ_{ij}-Kronecker's delta, β^*- HTT parameter.

The equations (1) - (5) reduces to the following cases

$K_1 = \tau_0 = 0$ Coupled theory of thermoelasticity (1980),
$K_1 = 0$ Lord - Shulman (L-S) (1967),
$K^* = \tau_0 = 0$Green-Naghdi–II (GN-II) (1993),
$\tau_0 = 0$ Green-Naghdi–III (GN-III) (1992).

3 Formulation and Solution of the Problem

A domain of thermoelastic half- space under the MGT thermoelastic model is taken into account under non-local and HTT impact is considered as the region $x_3 \geq 0$, which is homogenous and isotropic. The two-dimensional problem is in the plane ($x_1 - x_3$), which is subjected to normally distributed force and Ramp type thermal source in addition to the heat source in the form of laser pulse decaying with time and moving with constant velocity in one direction is considered, therefore with these consideration, we have:

$$\vec{u} = (u_1, 0, u_3) \ . \tag{6}$$

Dimensionless quantities are:

$$t'_{3i} = \frac{1}{\beta T_0} t_{3i}, \quad a' = \frac{\omega_1^2}{c_1^2} a, \quad \xi_1{}' = \frac{w_1}{c_1} \xi_1,$$
$$(\phi', T') = \frac{1}{T_0}(\phi, T), \quad (x_i', u'_i) = \frac{\omega_1}{c_1}(x_i, u_i),$$
$$(t', \tau_0') = \omega_1(t, \tau_0), \quad \beta^{*'} = \frac{1}{c_1^2}\beta^*,$$
$$F_1' = \frac{1}{\beta_1 T_0} F_1, \quad F_2' = \frac{c_1}{\omega_1 T_0} F_2 \quad (i = 1, 3), \tag{7}$$

where
$c_1^2 = \left(\frac{\lambda+2\mu}{\rho}\right)$ and $\omega_1^2 = \left(\frac{\rho C_e c_1^2}{K^*}\right)$.

Equations (1) - (5) by taking into account (6) and (7) determine:

$$a_1 \frac{\partial e}{\partial x} + a_2 \nabla^2 u_1 - a_3 \frac{\partial T}{\partial x} = (1 - \xi_1^2 \nabla^2) \frac{\partial^2 u_1}{\partial t^2}, \tag{8}$$

$$a_1 \frac{\partial e}{\partial z} + a_2 \nabla^2 u_3 - a_3 \frac{\partial T}{\partial z} = (1 - \xi_1^2 \nabla^2) \frac{\partial^2 u_3}{\partial t^2}, \tag{9}$$

$$\left(1 + \tau_0 \frac{\partial}{\partial t}\right)\left(\frac{\partial^2 T}{\partial t^2} + a_4 \frac{\partial}{\partial t^2} \nabla^2 q - \frac{\partial Q}{\partial t}\right) = \left(\frac{\partial}{\partial t} + a_5\right) \nabla^2 \phi \tag{10}$$

$$T = (1 - a\nabla^2)\phi, \tag{11}$$

$$\ddot{\phi} - \ddot{T} = \beta^* \nabla^2 \phi, \tag{12}$$

$$t_{33} = b_1 \frac{\partial u_1}{\partial x_1} + b_2 \frac{\partial u_3}{\partial x_3} - T, \tag{13}$$

$$t_{31} = b_3 \left(\frac{\partial u_3}{\partial x_1} + \frac{\partial u_1}{\partial x_3}\right), \tag{14}$$

where
$a_1 = \frac{\lambda+\mu}{\rho c_1^2}$, $a_2 = \frac{\mu}{\rho {c_1}^2}$, $a_3 = \frac{\beta_1 T_0}{\rho c_1^2}$,
$a_4 = \frac{\beta_1 c_1}{K^* \omega_1}$, $a_5 = \frac{K_1}{K^* \omega_1}$, $b_1 = \frac{\lambda}{\beta_1 T_0}$,
$b_2 = \frac{\lambda+2\mu}{\beta_1 T_0}$, $b_3 = \frac{\mu}{\beta_1 T_0}$.

Equations (8) - (11) are decoupled by using the dimensionless form of potential functions q and ψ as :

$$u_1 = \frac{\partial q}{\partial x_1} - \frac{\partial \psi}{\partial x_3}, \; u_3 = \frac{\partial q}{\partial x_3} + \frac{\partial \psi}{\partial x_1}. \tag{15}$$

Laplace and Fourier transforms are taken as:

$$\left.\begin{aligned} &\hat{f}(x_1, x_3, s) = \int_0^\infty e^{-st} f(x_1, x_3, t)\, dt \\ &\text{and} \\ &\tilde{f}(\xi, x_3, s) = \int_{-\infty}^{\infty} e^{-i\xi x_1} \hat{f}(x_1, x_3, s)\, dx_1 \end{aligned}\right\} \tag{16}$$

Applying (16) on (12) gives,

$$\tilde{T} = \tilde{\phi} - \varsigma\left(\frac{\partial^2}{\partial x_3^2} - \xi^2\right), \tag{17}$$

where

$$\varsigma = \begin{cases} 0 for 1T \\ a for TT \\ \dfrac{\beta^*}{s^2} for HTT \end{cases}$$

Equation (8) - (10) in the accompany of (15) - (17) yield the resulting expressions (suppressing the primes for convenience) after some algebraic calculation as:

$$\left(B_1 \frac{d^4}{dx_3^4} + B_2 \frac{d^2}{dx_3^2} + B_3\right)(\tilde{q}, \tilde{\phi}) = \left(B_4 \frac{d^2}{dx_3{}^2} + B_5\right)\tilde{Q} \tag{18}$$

$$\left(\frac{d^2}{dx_3^2} - \lambda_3^2\right)\tilde{\psi} = 0 \ , \tag{19}$$

where
$B_1 = R_2 R_6 - R_3 R_8$,
$B_2 = (R_1 R_6 + R_2 R_7 - R_8 R_4 - R_9 R_3)$,
$B_3 = (R_1 R_7 - R_9 R_4)$, $B_4 = R_5 R_8, B_5 = R_5 R_9$,
$R_1 = (1 + \tau_0 s)[s^2(1 + \varsigma\xi^2) + (s + a_5)\xi^2]$,
$R_2 = -(s^2 \varsigma(1 + \tau_0 s) + s + a_5)$,

$R_3 = a_4 s^2(1+\tau_0 s)$,
$R_4 = -a_4 s^2 \xi^2 (1+\tau_0 s)$,
$R_5 = s(1+\tau_0 s)$,
$R_6 = 1+\xi_1^2 s^2$,
$R_7 = -(s^2(1+\xi_1^2\xi^2)+\xi^2)$,
$R_8 = a_3 \varsigma$,
$R_9 = -a_3(1+\varsigma\xi^2)$.

The bounded solution of equation (18) and (19) i.e. $\tilde{q}, \tilde{\psi}, \tilde{\phi} \to 0$ as $x_3 \to \infty$ can be expressed as:

$$\tilde{q} = A_1 e^{-\lambda_1 x_3} + A_2 e^{-\lambda_2 x_3} + \frac{R_5 R_9}{R_1 R_7 - R_9 R_4}\hat{Q}, \quad (20)$$

$$\tilde{\phi} = d_1 A_1 e^{-\lambda_1 x_3} + d_2 A_2 e^{-\lambda_2 x_3} + d_3 \hat{Q}, \quad (21)$$

$$\tilde{\psi} = A_3 e^{-\lambda_3 x_3}, \quad (22)$$

where

$d_i = -\frac{\lambda^2{}_i R_6 + R_7}{R_9 + R_8 \lambda_i^2}$, $d_3 = \frac{R_5 R_7}{R_1 R_7 - R_9 R_3}$, where $i = 1,2$

$\lambda_l (l = 1,2)$ being the roots of the characteristic equation $\left(B_1 \frac{d^4}{dx_3^4} + B_2 \frac{d^2}{dx_3^2} + B_3\right) = 0$.

3.1 Heat Source

Let the physical entities be affected by a moving heat source which is assumed to be in non-dimensional form:

$$Q = Q_0 \, exp\left(-\frac{t}{t_p}\right)\delta(x_1 - vt), \quad (23)$$

where Q_0 is constant, $t_p$is the time duration of laser pulse decaying, v is the moving heat source, t is time, $\delta(\,)$ is the Dirac delta function.

4 Boundary Conditions

Here, we explore the impact of normal distributed force and Ramp type thermal sources as:

$$(i)t_{33} = F_1(x_1, t) \quad (ii)t_{31} = 0 \quad (iii)\frac{\partial \phi}{\partial x_3} = F_2(x_1, t) \quad \text{at } x_3 = 0 \quad (24)$$

where

$$F(x_1, t) = F_{10}\begin{cases} sin\frac{\pi t}{\eta}\delta(x) & 0 \le t < \eta \\ 0 & t > \eta \end{cases},$$

$$F_2(x,t) = F_{20}\delta_{t_0}(t)\delta(x),$$

$$\delta_{t_0}(t) = \begin{cases} \frac{t}{t_0} & 0 \le t < t_0 \\ 0 & t > t_0 \end{cases}. \quad (25)$$

F_{10} is the magnitude of force, F_{20} is the constant temperature applied on the boundary.

Invoking (16) on (23)-(25), we have

$$(i)\tilde{t}_{33} = \tilde{F}_1(\xi, s) \quad (ii)\tilde{t}_{31} = 0 \quad (iii)\ \frac{\partial \tilde{\phi}}{\partial x_3} = \tilde{F}_2(\xi, s) \quad \text{at } x_3 = 0 \quad (26)$$

where

$$\tilde{F}_1(\xi, s) = \frac{F_{10}\,\pi\,\eta(1-e^{-s\eta})}{\pi^2 + s^2\eta^2}, \quad \tilde{F}_2(\xi, s) = \frac{F_{20}(1-e^{-st_0})}{t_0 s},$$

$$\tilde{Q} = Q_0 e^{-\left(s+\frac{1}{tp}\right)\frac{x_1}{v}} \quad (27)$$

Invoking (16) -(17) (after suppressing the primes) in (13) -(14) along with (20) -(22), the expressions of displacements, stresses, conductive temperature, and thermodynamic temperature are obtained by considering the boundary conditions defined by (26) -(27) as:

$$\tilde{u}_1 = \frac{1}{\Delta}\begin{bmatrix} F_{10}\left[(-\iota\xi)\sum_{i=1}^{2}\Delta_{i1}\, e^{-\lambda_i x_3} + \Delta_{31} e^{-\lambda_3 x_3}\right] + F_{20}\left[(-\iota\xi)\sum_{i=1}^{2}\Delta_{i2} e^{-\lambda_i x_3} + \Delta_{32}\, e^{-\lambda_3 x_3}\right] \\ -i\xi\left(\sum_{i=1}^{2}\Delta_{i3}\, e^{-\lambda_i x_3} - \frac{R_5 R_7 \Delta \hat{Q}}{R_1 R_7 - R_9 R_4}\right) + \Delta_{33} e^{-\lambda_3 x_3} \end{bmatrix} \quad (28)$$

$$\tilde{u}_3 = \frac{-1}{\Delta}\begin{bmatrix} F_{10}\left(\sum_{i=1}^{2}\lambda_i \Delta_{i1}\, e^{-\lambda_i x_3} + i\xi\Delta_{31} e^{-\lambda_3 x_3}\right) + F_{20}\left(\sum_{i=1}^{2}\lambda_i \Delta_{i2}\, e^{-\lambda_i x_3} + i\xi\Delta_{32} e^{-\lambda_3 x_3}\right) \\ +\left(\sum_{i=1}^{2}\lambda_i \Delta_{i3}\, e^{-\lambda_i x_3} + i\xi\Delta_{33} e^{-\lambda_3 x_3}\right) \end{bmatrix} \quad (29)$$

$$\hat{t}_{33} = \frac{1}{\Delta}\left[F_{1_0}\sum_{i=1}^{3} H_i\, \Delta_{i1} e^{-\lambda_i x_3} + F_{20}\sum_{i=1}^{3} H_i \Delta_{i2}\, e^{-\lambda_i x_3} + \sum_{i=1}^{3} H_i \Delta_{i3} e^{-\lambda_i x_3} + H_4 b_4 \Delta\right] \quad (30)$$

$$\hat{t}_{31} = \frac{1}{\Delta}\left[F_{1_0}\sum_{i=1}^{3} H_{i+4}\Delta_{i1}\, e^{-\lambda_i x_3} + F_{20}\sum_{i=1}^{3} H_{i+4}\Delta_{i2} e^{-\lambda_i x_3} + \sum_{i=1}^{3} H_{i+4}\Delta_{i3} e^{-\lambda_i x_3}\right] \quad (31)$$

$$\hat{\phi} = \frac{1}{\Delta}\left[F_{1_0}\sum_{i=1}^{2} H_{i+7}\Delta_{i1} e^{-\lambda_i x_3} + F_{20}\sum_{i=1}^{2} H_{i+7}\Delta_{i2} e^{-\lambda_i x_3} + \sum_{i=1}^{2} H_{i+7}\Delta_{i3} e^{-\lambda_i x_3} + H_{10} b_4\right] \quad (32)$$

$$\hat{T} = \frac{1}{\Delta}\left[F_{1_0}\sum_{i=1}^{2} d_i \Delta_{i1}\, e^{-\lambda_i x_3} + F_{20}\sum_{i=1}^{2} d_i \Delta_{i2}\, e^{-\lambda_i x_3} + \sum_{i=1}^{2} d_i \Delta_{i3}\, e^{-\lambda_i x_3} + d_3 b_4\right] \quad (33)$$

where
$\Delta = d_1(H_2H_7 - H_3H_6) + d_2(H_3H_5 - H_1H_7)$,
$\Delta_{11} = -d_2H_7b_5$, $\Delta_{12} = (H_2H_7 - H_3H_6)b_6$,
$\Delta_{13} = (H_4H_7d_2 + H_3H_6d_3 - H_2H_7d_3)b_4$,
$\Delta_{21} = d_1H_7b_5$,
$\Delta_{22} = (H_3H_5 - H_1H_7)b_6$,
$\Delta_{23} = (H_1d_3 - H_4d_1)H_7b_4$,
$\Delta_{31} = (d_2H_5 - d_1H_6)b_5$,
$\Delta_{32} = (H_1H_6 - H_2H_5)b_6$,
$\Delta_{33} = (H_2H_5d_3 - H_1H_6d_3 - H_4H_5d_2H_4H_6d_1)b_4$,
$H_i = -b_1\xi^2 + b_2\lambda_i^2 - (1 + \varsigma\xi^2)d_i + \varsigma d_i\lambda_i^2$,
$H_3 = \lambda_3 i\xi(b_1 + b_2)$, $H_4 = \frac{-R_5R_9}{R_1R_7+R_9R_3}$,
$H_{i+4} = -ib_3\xi\lambda_i$, $H_{i+7} = d_i\left(1 + \varsigma\xi^2 - \varsigma\lambda_i^2\right)$,
$H_7 = -b_3\lambda_3$, $H_{10} = d_3(1 + \varsigma\xi^2)$,
$b_4 = Q_0e^{-\left(s+\frac{1}{t_p}\right)\frac{x_1}{v}}$, $b_5 = \frac{\pi\eta(1+e^{-\eta s})}{\pi^2+s^2\eta^2}$,
$b_6 = \frac{1-e^{-st_0}}{st_0}$ $i = 1,2.$

5 Special Cases

1. **MGT thermoelasticity with HTT**: let $\xi_1 \to 0$ in equations (28)-(33), determine the resulting expressions for MGT with HTT.
2. **Non Local Lord Shulman Model (L-S model) with HTT**: Substituting $K_1 = 0$ in equations (28)-(33), gives the expression of generalized thermoelasticity which involves one relaxation time under nonlocal and HTT.
3. **Green- Naghdi-II model (GN-II model) with HTT**: if $K^* = \tau_0 = 0, K_1 > 0$ in equations (28)-(33) will explore the resulting quantities for GN type-II model under non local theory and HTT.
4. **Green- Naghdi-III model (GN-III model) with HTT**: i.f $K^*, K_1 > 0$, $\tau_0 = 0$ in equations (28)-(33), determines expressions for GN type - III model under the influence of nonlocal and HTT.

Sub cases:

5. 1 if $\varsigma = a$: We obtain the results for MGT thermoelasticity with two temperatures along with non-local effect.

5. 2. if $\varsigma = 0$: We attain the results for MGT thermoelasticity with one temperature along with non-local effect.

6 Inversion of the Transforms

The components of displacement, stresses, temperature distribution, and conductive temperature are the functions of s, $x_3$and ξwhich are parameters of the Laplace transform and Fourier transform respectively. To invert these quantities into the physical domain, we invert the transforms by applying the method explained by [27].

7 Numerical Result and Discussion

To explore the impact of various parameters under the assumed model, the numerical calculations are made for five different cases, (i) nonlocal, (ii) moving heat source and (iii) hyperbolic two temperature, (iv) normal distributed forces (v) Ramp type thermal sources for MGL theory of thermoelasticity.

Following, [28], we take the case of magnesium crystal, the physical constants used are:
$\lambda = 2.17 \times 10^{10}Nm^{-2}, \mu = 3.278 \times 10^{10}Nm^{-2}$,
$K^* = 1.7 \times 10^2Wm^{-1}\deg^{-1}$, $\omega_1 = 3.58.10^{11}S^{-1}$,
$\beta_1 = 2.68.10^6Nm^{-2}\deg^{-1}, \rho = 1.74.10^3Kgm^{-3}$,
$C_e = 1.04.10^3JKg^{-1}\deg^{-1}$ $T_0 = 298k, t_p = 2s$
and non- dimensional relaxation times are taken as $\tau_0 = .03s$.

7.1 Non-Local Effect

In this case, we consider non-local parameters as $\xi_1 = 0.75$, $\xi_1 = 0.50$, $\xi_1 = 0.20$ and $\xi_1 = 0$, HTT parameter $\varsigma = 0.5$and $v = 1$ for the range $0 \le x_1 \le 10$. The solid line correspond to ($\xi_1 = 0.75$), small dashed line corresponds to ($\xi_1 = 0.50$) whereas, solid line with center symbol $\diamond$ correspond to ($\xi_1 = 0.20$) and small dashed line with center symbol represents the case of ($\xi_1 = 0$).

7.1.1 Normal Distributed Force

Figure 1 (Appendix) shows the behavior of t_{33} vs x_1. It is noticed that the behavior of t_{33} for $\xi_1 = 0.75$ and $\xi_1 = 0.50$, is opposite in nature as that of $\xi_1 = 0.20$ and $\xi_1 = 0$ for the range $0 \le x_1 \le 2$ and $6 \le x_1 \le 10$ respectively, while similar trends are noticed in the left over interval. It is also seen that near the boundary surface, t_{33} attains minima for $\xi_1 = 0.20$at $x_1 = 4$.

Figure 2 (Appendix) is a plot of t_{31}vs x_1, which demonstrates that for $\xi_1 = 0.0$, the values of $t_{31}$are higher in contrast to those obtained for $\xi_1 = 0.20$for

the entire range. It is also seen that for a higher value ($\xi_1 = 0.75$, $\xi_1 = 0.50$), the values increase in the entire range with a significant difference in their magnitude.

Figure 3 (Appendix) predicts T vs x_1. It is seen that the T for intermediate value of non-local parameter ($\xi_1 = 0.50$, $\xi_1 = 0.20$) are opposite in nature to those for the value of ξ_1 ($\xi_1 = 0.75$,$\xi_1 = 0.0$), it is also noticed that the magnitude of values of T for $\xi_1 = 0.50$ is higher as compared to other considered values of non-local parameter.

The graphical representation of ϕ with x_1 is represented in Figure 4 (Appendix). It is noticed that ϕ exhibits sa imilar pattern in the range $0 \le x_1 \le 2$ and $4 \le x_1 \le 6$ for ξ_1 ($\xi_1 = 0.75$, $\xi_1 = 0.0$), whereas ϕ shows an reverse trend for other considered v values of ξ_1, which is accounted as the impact of non-local parameter.

7.1.2 Ramp Type Thermal Source

Figure 5 (Appendix) represents the variations of t_{33} vs x_1. t_{33} begins with large value in the absence of non-local parameter. As the value of non-local parameter increases the value of t_{33} increases and attain maxima at$x_1 = 5$ for $\xi_1 = 0.75$.

The plot of t_{31}vs x_1 is represented by Figure 6 (Appendix). It is seen that the trend of t_{31} for $\xi_1 = 0.20$and $\xi_1 = 0.0$ are inverse in nature in the entire range, whereas for higher values of ξ_1 ($\xi_1 = 0.50$, $\xi_1 = 0.75$) are similar in nature in the entire range, magnitude of values are greater for higher value of ξ_1.

Figure 7 (Appendix) shows the variations of T vs x_1. It is noticed that T exhibits oscillatory behavior for all values of ξ_1, the magnitude of oscillation is greater in the absence of non-local parameter i.e. $\xi_1 = 0$, while for other values of ξ_1 , T shows small variations about ' 2 '.

Figure 8 (Appendix) exhibits the plot for ϕ vs x_1. The trend of ϕ is similar to that for T with significant difference in their magnitude.

7.2 Moving Heat Source

In this case, we consider moving heat source parameter $v = 1.75$, $v = 1$ and $v = 0.25$, non-local parameter $\xi_1 = 0.50$and hyperbolic two-temperature parameter $\varsigma = 0.5$ for the range $0 \le x_1 \le 10$. The solid line corresponds to ($v = 1.75$), the small dashed line corresponds to ($v = 1$) and the long dashed line represents the case of $v = 0.25$.

7.2.1 Normal Distributed Force

Figure 9 (Appendix) demonstrates the variations of t_{33} vs x_1. It is noticed that the value of t_{33} decreases for the range $2 \le x_1 \le 3$ and $6 \le x_1 \le 10$ and increases in the rest of interval of for all values of v. It is also noticed that the magnitude of values for t_{33} are higher for greater value of v ($v = 1.75$).

The variation of t_{31} vs x_1 is represented in Figure 10 (Appendix). t_{31} shows an increasing trend for the entire range for all values of v. It is also revealed that the magnitude of the values of t_{31} is greater for larger values of v.

Figure 11 (Appendix) depicts the trend of T vs x_1. The value of temperature T begins with large value for velocity, $v = 0.25$ for interval $0 \le x_1 \le$ 2and for left over interval, T follows an oscillatory behavior. The magnitude of oscillation is higher in case of $v = 1.75$ than other considered value of v.

The graphical presentation of ϕ vs x_1 is represented in Figure 12 (Appendix). ϕ follows an oscillatory behavior for all values of v for the entire range, the magnitude of oscillation is greater for higher values of v.

7.2.2 Ramp Type Thermal Source

Figure 13 (Appendix) depicts the variations of t_{33} vs x_1 . The values of t_{33} for $v = 1.75$ and $v = 1$ increases for the range $0 \le x_1 \le 6$, magnitude of values for $v = 1.75$ are greater in comparison to those for $v = 1$ and decreases in left over interval, whereas the smaller value of for v ($v = 0.25$), t_{33} shows a steady state about the origin.

Figure 14 (Appendix) is a plot of t_{31} vs x_1. It is evident from the plot that t_{31} follows an oscillatory behavior for all values of v, the magnitude of oscillation is higher for a greater value of v ($v =$ 1.75).

Figure 15 (Appendix) exhibits the plot for T vs x_1. The value of T for $v = 1.75$ and $v = 1$decreases for the range $3 \le x_1 \le 5$ and $8 \le x_1 \le 10$, and increases for the left over interval, whereas for $v =$ 0.25, the values of T exhibit small variations about the value 2.

Figure 16 (Appendix) is a plot of ϕ vs x_1. The behavior of ϕ is similar in nature as observed for T with a significant difference in their magnitude, which reveals the impact of two temperature parameters.

7.3 Hyperbolic Two Temperature

In this case, we consider hyperbolic two temperature parameter $\varsigma = 0.75$, $\varsigma = 0.50$ and two temperature parameter $a = 0.104$ and $a = 0.0$, non-local parameter $\xi_1 = 0.20$ and moving heat source $v = 1$ for the range $0 \le x_1 \le 10$. The solid line corresponds to ($\varsigma = 0.75$), small dashed line corresponds to ($\varsigma = 0.50$) whereas, the solid line with the center symbol ⋄ correspond to ($a = 0.104$) and small dashed line with center symbol *o*represents the case of ($a = 0.0$).

7.3.1 Normal Distributed Force

It is evident from Figure 17 (Appendix), which is a plot of t_{33} vs x_1 that the trend of t_{33} are similar in nature for higher value HTT ($\varsigma = 0.75, \varsigma = 0.50$) in the entire interval except in the range $7 \le x_1 \le 10$ with a magnitude of values is higher for smaller value of hyperbolic two temperature parameter for $\varsigma = 0.50$, whereas in case of TT ($a = 0.104$) and $a = 0.0$ trend of t_{33} are similar in nature in the first half of the interval, whereas opposite behavior in the rest of the interval.

Figure 18 (Appendix) is a plot of t_{31} vs x_1. It is noticed that the values of t_{31} for show a decreasing trend in the entire interval, whereas the values of t_{31} for $a = 0.104$ and $a = 0.0$ increases in the range $0 \le x_1 \le 7$ and decreases in the remaining range. It also seen that the value of t_{31} for $\varsigma = 0.75$ shows a small variation about the value '-1' and ultimately approaches zero.

Figure 19 (Appendix) shows the variations of T vs x_1. It is noticed that the trend of T for HTT i.e. $\varsigma = 0.75$ is opposite in nature as observed for the case of TT ($a = 0.104$) in the entire range, which shows a significant impact of hyperbolic two temperature parameters. It is also noticed that the trend of T in the absence of two temperature parameters are reverse in nature as for the case of HTT i.e. $\varsigma = 0.50$.

Figure 20 (Appendix) is a plot of ϕ vs x_1. ϕ shows an oscillatory trend in the entire range. It is observed that the magnitude of oscillation is higher for HTT ($\varsigma = 0.75$) as compared to other considered values of HTT parameter.

7.3.2 Ramp Type Thermal Source

Figure 21 (Appendix) is a plot of t_{33} vs x_1. The values of t_{33} increase for the entire range for HTT parameter ($\varsigma = 0.75$ and $\varsigma = 0.50$), magnitude of values for $\varsigma = 0.50$ are greater as compared to those for $\varsigma = 0.75$. Also, the values of t_{33} for $a = 0.104$ and $a = 0.0$ decreases in the range $3 \le x_1 \le 7$ and reverse trend is noticed in the left-over interval.

Figure 22 (Appendix) is a plot of t_{31} vs x_1. t_{31} for $a = 0.0$ shows the opposite trend as compared to other considered cases for the first half of the interval, which accounted for as significant effect of two temperature parameters. In the latter half of the interval, the values of show an oscillatory behavior.

Figure 23 (Appendix) is a plot of T vs x_1. T shows opposite behavior as compared to other considered values of HTT parameters for the entire range. In the absence of two temperature parameters T shows a steady state for the interval $0 \le x_1 \le 4$ and later on the values of *T* decrease for the interval $4 \le x_1 \le 6$, $8 \le x_1 \le 10$ and increase in the left-over interval.

Figure 24 (Appendix) is a plot of ϕ vs x_1. The variation of ϕ shows a similar trend as for T with significant differences in their magnitude, which reveals the impact of HTT and two temperature parameters.

8 Conclusion

In this work, we considered a thermomechanical problem based on the MGT model having non-local, Ramp type heat source and hyperbolic two temperature effects. The paper presents an analytic solution for the thermomechanical behavior of the deformation problem in which an infinite body is subjected to the heat source in the form of a laser pulse decaying with time and moving with constant velocity in one direction. The problem is further examined with normal distributed force and ramp type thermal source**.** The results are displayed graphically to illustrate the effect of nonlocal parameters, moving heat source parameters and impact of hyperbolic two temperatures. The following observations are obtained from numerical computed results:

- when normal distributed force is applied, it is observed that trends of $t_{33}$and t_{31} for$\xi_1 = 0.75$, $\xi_1 = 0.50$ are opposite in nature as observed for $\xi_1 = 0.20$ and $\xi_1 = 0$. It is also observed that T and ϕ shows oscillatory behavior, the magnitude of oscillation is higher for $\xi_1 = 0.50$.

- In case of Ramp type thermal source, the value of t_{33} increases in most of the interval for all values of ξ_1, while t_{31}, T and ϕ shows oscillatory behavior in the entire range, the magnitude of oscillation is higher in the absence of non-local parameter.
- It is observed that a higher value of the moving heat source parameter enhances the value of t_{33}, T and ϕ for normal distributed force as well as for Ramp type thermal source. It is also observed that the behavior of variation for t_{33}, t_{31}, T and $\phi$for different values of v are similar in nature with differences in their magnitude of oscillations.
- The hyperbolic two temperature effect enhances the magnitude of T and ϕ in contrast to t_{33} and t_{31}. It is also noticed that in most of the range, the behavior of all entities for a higher value of hyperbolic two temperature parameters i.e $\varsigma = 0.75$ are opposite in nature as observed for two temperature parameter $(a = 0.104)$ and for classical one temperature $(a = 0.0)$ for normally distributed force as well as for Ramp type thermal source.

The physical applications of the model can be found in mechanical engineering and geophysics.

References:

[1] H. W. Lord and Y. Shulman, A generalizeddynamical theory of Solid, *J. Mech. Phys.*, Vol.15, No.5, 1967, pp. 299–309, https://doi.org/10.1016/0022-5096(67)90024-5

[2] A. E.Green and K.A.Lindsay,Thermoelasticity, *J. Elast.,* Vol.2, No.1, 1972, pp. 1–7, https://doi.org/10.1007/BF00045689

[3] A. E. Green and P.M. Naghdi,A re-examination of the basic postulates of thermomechanics, *Proc. R. Soc. Lond.,* Vol.432, No.1885, 1991, pp. 171–194, https://doi.org/10.1098/rspa.1991.0012

[4] A. E. Green and P.M. Naghdi, On undamped heat waves in an elastic solid, *J. Therm.* Stresses, Vol.15, No.2, 1992, pp. 253-264, https://doi.org/10.1080/01495739208946136

[5] A. E. Green and P.M. Naghdi, Thermoelasticity without energy dissipation, *J. Elast.,* Vol.31, No.3, 1993, pp. 189-208, https://doi.org/10.1007/BF00044969

[6] A. E. Green and P.M. Naghdi,A re-examination of the base postulates of thermomechanics, *Proceedings of Royal Society London A*, Vol.432,1985, pp.171 -194, https://doi.org/10.1098/rspa.1991.0012

[7] P J Chen and M E Gurtin, On a theory of heat conduction involving two-temperatures, *Journal of Applied Mathematics and Physics (ZAMP)*, Vol. No.19, 1968, pp. 614-627, https://doi.org/10.1007/BF01594969

[8] P J Chen, M E Gurtin, and W O Williams, On the thermodynamics of non-simple elastic materials with two temperatures, *Journal of Applied Mathematics and Physics (ZAMP)*, Vol.20, 1969, pp. 107-112, https://doi.org/10.1007/BF01591120

[9] H M Youssef, Theory of two-temperature-generalised thermoelasticity, *IMA Journal of Applied Mathematics*, Vol.71,No.3, 2006, pp.383 -390, https://doi.org/10.1093/imamat/hxh101

[10] H M Youssef, A A El-Bary, Theory of hyperbolic two-temperature generalized thermoelasticity, *Mat. Phy. Mech.,* Vol.40, 2018, pp. 158-171, http://dx.doi.org/10.18720/MPM.4022018_4

[11] R Kumar, R. Prasad, and R Kumar, Thermoelastic interactions on hyperbolic two-temperature generalized thermoelasticity in an infinite medium with a cylindrical cavity, *Elsevier European Journal of Mechanics - A/Solids*, Vol. 82, 2020, https://doi.org/10.1016/j.euromechsol.2020.104007

[12] A Hobiny, Ibrahim Abbas and M. Marin, The influences of the hyperbolic Two-Temperatures theory on waves propagation in a semiconductor material containing spherical cavity, *Mathematics*, Vol.10, No.121, 2022, https://doi.org/10.3390/math10010121

[13] A.C.Eringen,Nonlocal polar elastic continua, *Int. J. Eng. Sci.*, Vol.10, 1972, pp. 1-16, https://doi.org/10.1016/0020-7225(72)90070-5

[14] A.C.Eringen,Theory of nonlocal thermoelasticity, *Int. J. Eng. Sci.* Vol.12, 1974, pp.1063 -1077, https://doi.org/10.1016/0020-7225(74)90033-0

[15] N. De Sarkar, and N.S. Sarkar, Waves in nonlocal thermoelastic solids of type II, *Journal of Thermal Stresses,* Vol.42, 2019, pp.1153 -1170,

https://doi.org/10.1080/01495739.2019.1618760

[16] F. S. Bayones, S. Mondal,S. M. Abo-Dahab and A. A. Kilany, Effect of moving heat source on a magneto-thermoelastic rod in the context of Eringen's nonlocal theory under three-phase lag with a memory dependent derivative, *Mechanics Based Design of Structures and Machines*, Vol. 10., 2021, https://doi.org/10.1080/15397734.2021.1901735

[17] T. Saeed and I. Abbas, Effects of the nonlocal thermoelastic Model in a thermoelastic nanoscale material, *Mathematics*, Vol.10, No.2, 2022, https://doi.org/10.3390/math10020284.

[18] R.Quintanilla,Moore-Gibson-Thompson thermoelasticity, *Math.Mech. Solids*, Vol.24, 2019, pp. 4020 -4031, https://doi.org/10.1177/1081286519862007.

[19] R. Quintanilla, Moore-Gibson-Thompson thermoelasticity with two temperatures, *Appl. Eng. Sci.*, Vol.1, 2020, https://doi.org/10.1016/j.apples.2020.100006.

[20] A. E. Abouelregal, I. E. Ahmed, M. E. Nasr, K. M. Khalil, A. Zakria, and F. A. Mohammed, Thermoelastic processes by a continuous heat source line in an infinite solid via Moore–Gibson–Thompson thermoelasticity, *Materials (Basel)*, Vol.13, No.19, 2020, pp. 1-17, https://doi.org/10.3390/ma13194463.

[21] M. Marin, M. I. A. Othman, A. R. Seadawy and C. Carstea, A domain of influence in the Moore–Gibson–Thompson theory of dipolar bodies, Journal of Taibah University for Science, Vol. 14, No.1, 2020, pp.653 -660, https://doi.org/10.1080/16583655.2020.1763664.

[22] K. Jangid, A domain of influence theorem under MGT thermoelasticity theory, *Sage Journals*, 2020, pp. 1-11, https://doi.org/10.1177/1081286520946820

[23] M. Pellicer and R. Quintanilla, On uniqueness and instability for some thermomechanical problems involving the Moore–Gibson–Thompson equation, *Journal of Applied Mathematics and Physics (ZAMP)*,Vol. 71, No.3, , 2020, https://doi.org/10.1007/s00033-020-01307-7.

[24] Abouelregal A. E., Hakan Ersoy, and Omer Civalek, Solution of Moore–Gibson–Thompson Equation of an Unbounded Medium with a Cylindrical Hole, *Mathematics*, Vol. 9, 2021, pp.1536, https://doi.org/10.3390/math9131536.

[25] K. Jangid, M. Gupta, and S. Mukhopadhyay, On propagation of harmonic plane waves under the Moore – Gibson–Thompson thermoelasticity theory, *Waves in Random and Complex Media*, 2021, https://doi.org/10.1080/17455030.2021.1949071.

[26] A. E. Abouelregal,Fractional derivative Moore-Gibson-Thompson heat equation without singular kernel for a thermoelastic medium with a cylindrical hole and variable properties, *ZAMM*, 2022, https://doi.org/10.1002/zamm.202000327.

[27] R. Kumar, S .Kaushal, L.S Reen, and S.K Garg, Deformation due to various sources in transversely isotropic thermoelastic material without energy dissipation and with two-temperature, *Materials physics and mechanics*, Vol. 27, No.1, 2016, pp.21 -31.

[28] R. S Dhaliwal, and A Singh, Dynamical Coupled Thermoelasticity, Hindustan Publishers, Delhi, India, (1980), [Online]. https://cir.nii.ac.jp/crid/1130282271727400448 (Accessed Date: March 13, 2024).

Contribution of Individual Authors to the Creation of a Scientific Article (Ghostwriting Policy)

- Rajneesh Kumar carried out visualization Conceptualization, Ideas and Supervision
- Sachin Kaushal carried out Conceptualization, and supervision, editing implemented the software
- Gulshan Sharma organized Writing - review and Resources and has implemented Program.

Sources of Funding for Research Presented in a Scientific Article or Scientific Article Itself

No funding was received for conducting this study.

Conflict of Interest

The authors have no conflicts of interest to declare.

APPENDIX

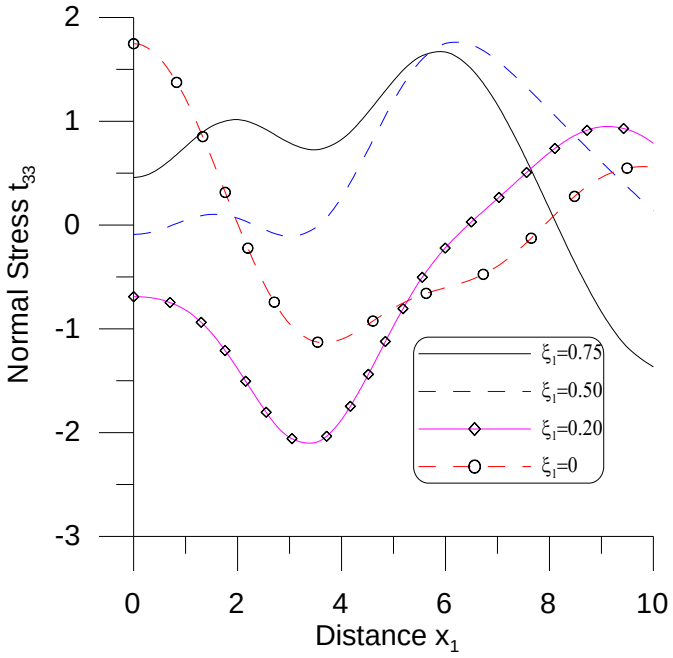

Fig. 1: Variation of t_{33} vs x_1
(Non local Parameter-Distributed Force)

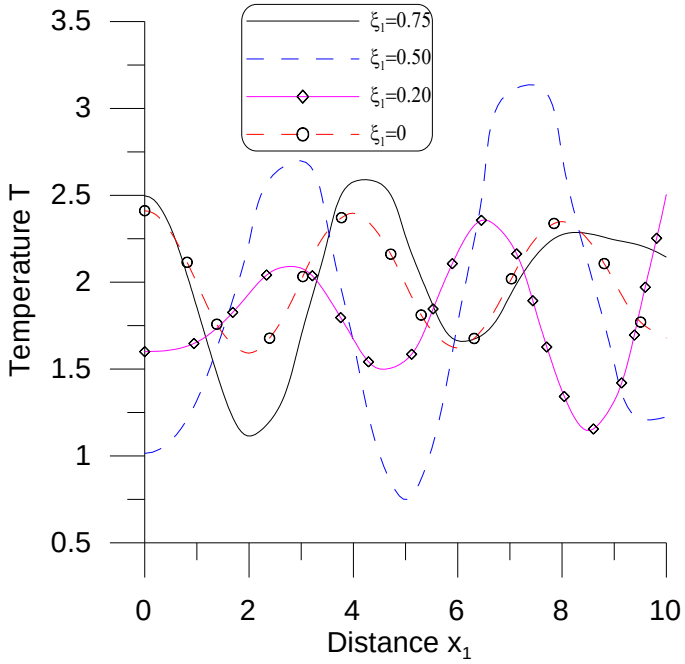

Fig. 3: Variation of T vs x_1
(Non-local Parameter-Distributed Force)

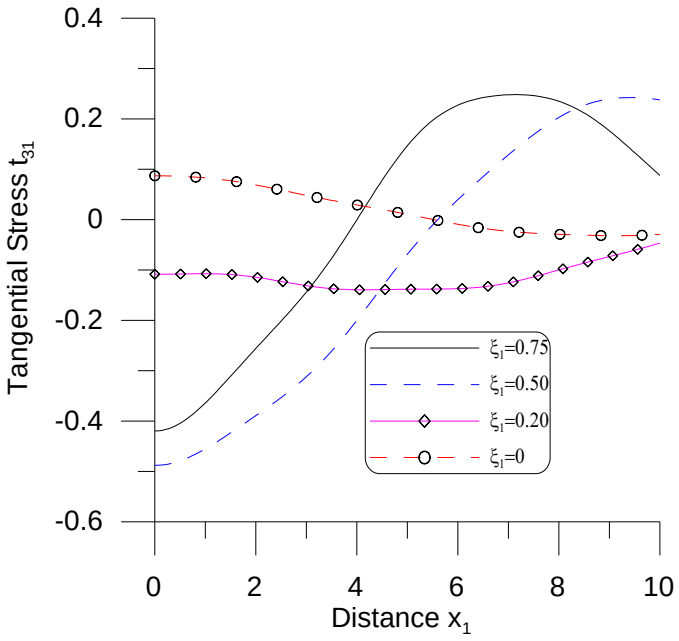

Fig. 2: Variation of t_{31} vs x_1
(Non local parameter-Distributed Force)

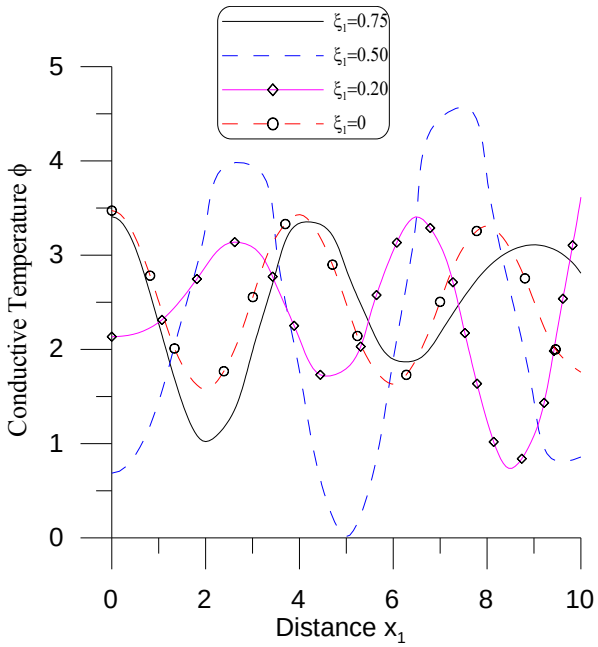

Fig. 4: Variation of ϕ vs x_1
(Non local parameter-Distributed Force)

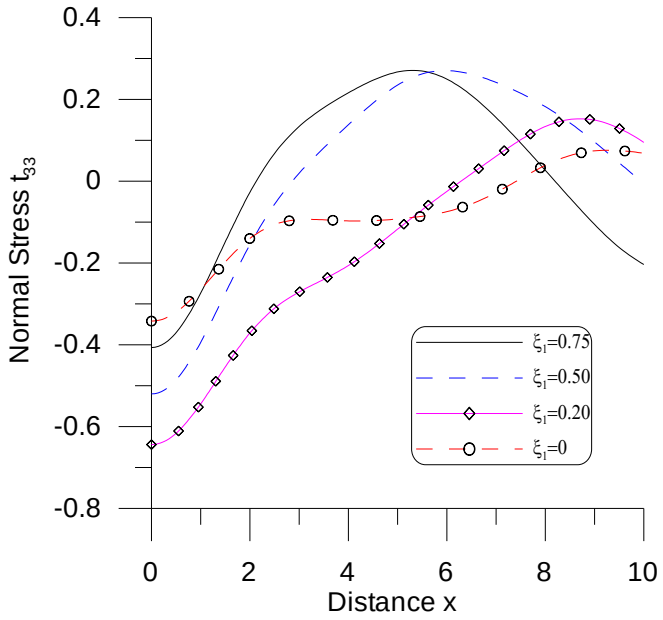

Fig. 5: Variation of t_{33} vs x_1 (Non local parameter - Thermal Source)

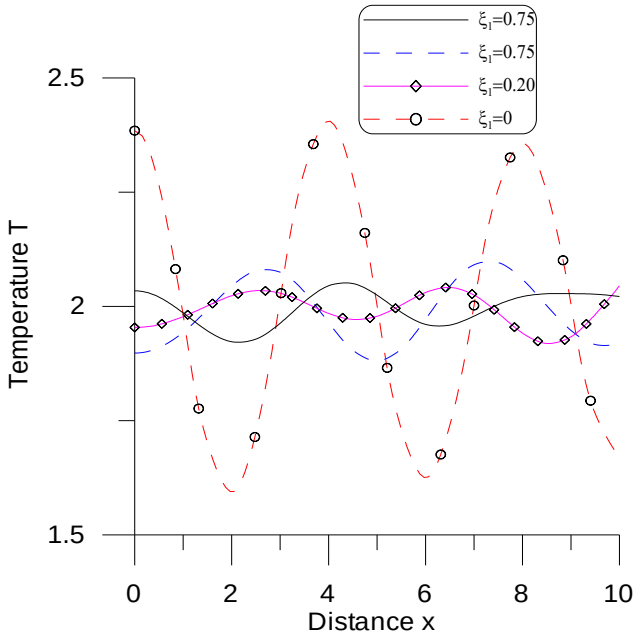

Fig. 7: Variation of T vs x_1 (Non local parameter- Thermal Source)

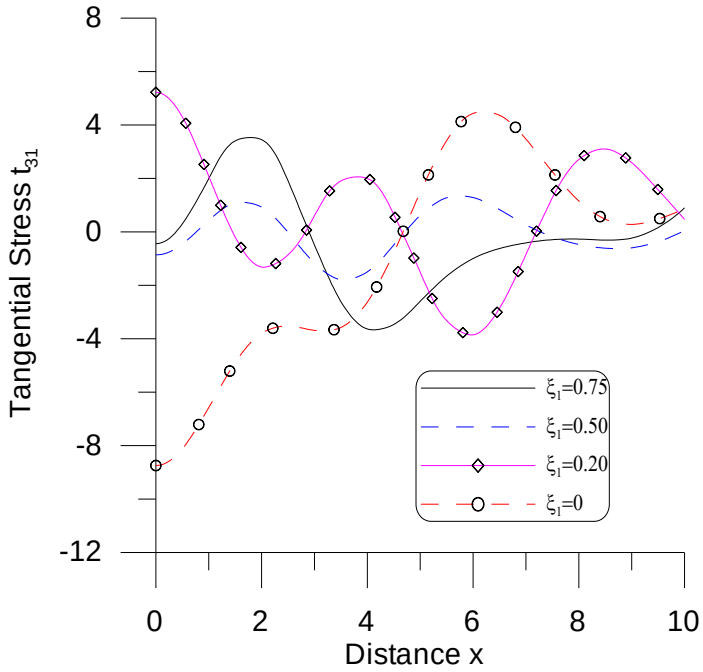

Fig. 6: Variation of t_{31} vs x_1 (Non local parameter-Thermal Source)

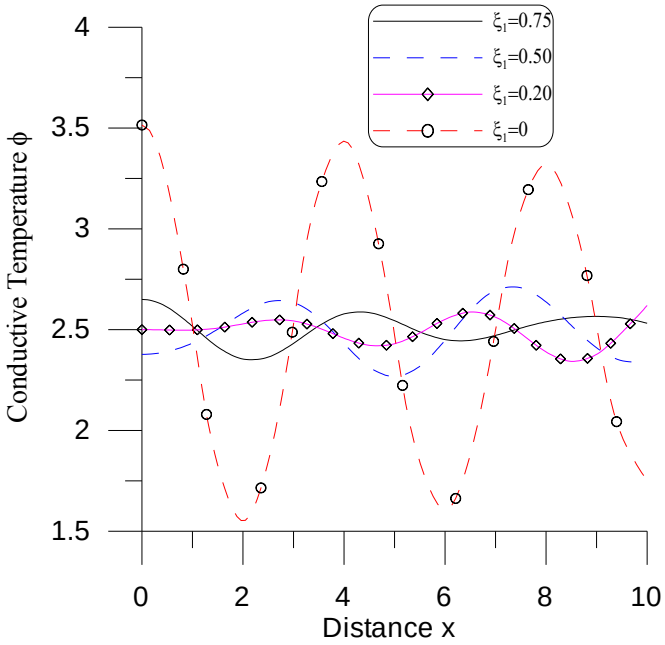

Fig. 8: Variation of ϕ vs x_1 (Non local parameter- Thermal Source)

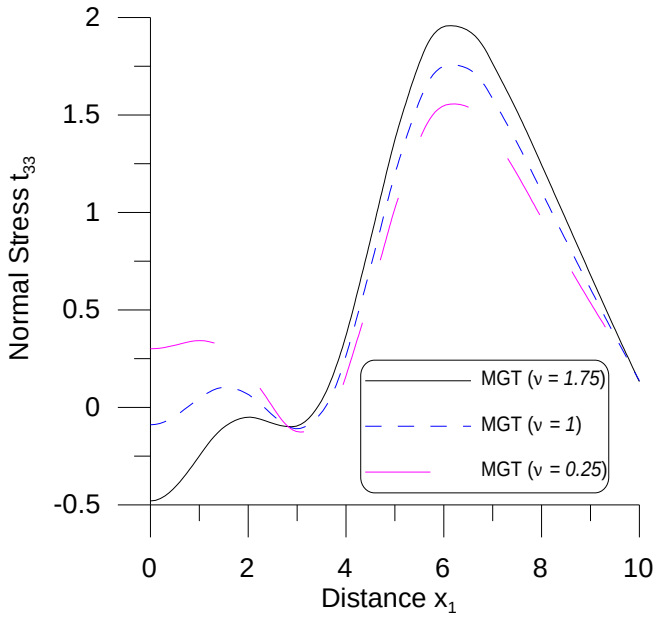

Fig. 9: Variation of t_{33} vs x_1
(Heat Source Velocity - Distributed Force)

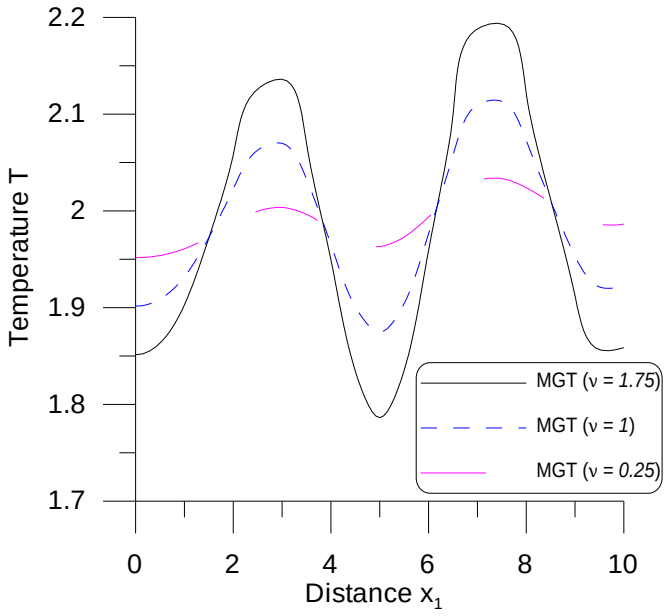

Fig. 11: Variation of T vs x_1
(Heat Source Velocity - Distributed Force)

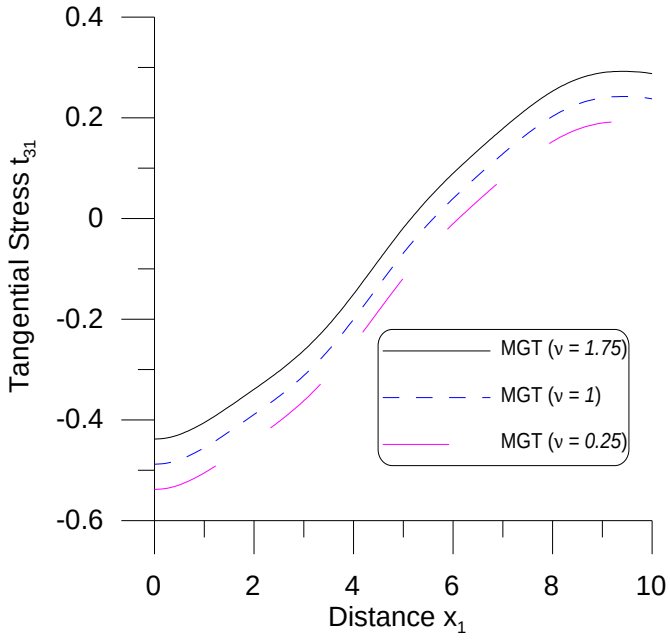

Fig. 10: Variation of t_{31} vs x_1
(Heat Source Velocity - Distributed Force)

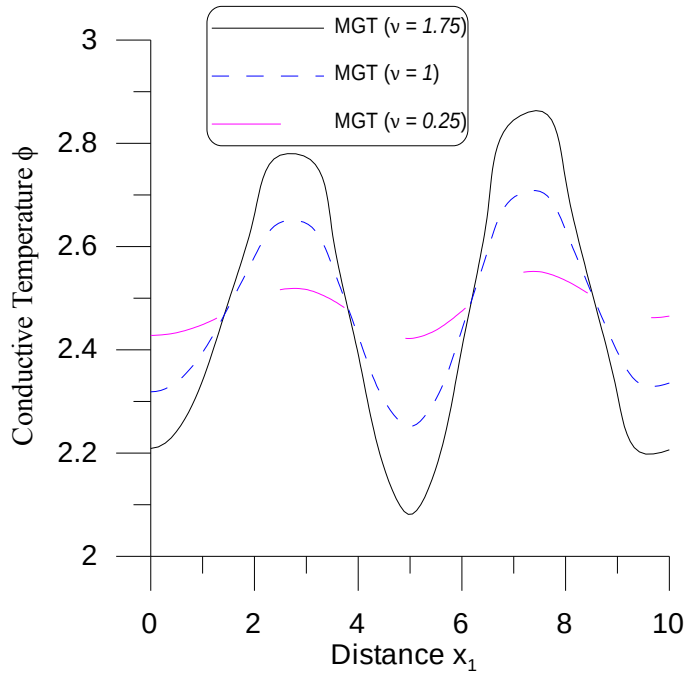

Fig. 12: Variation of ϕ vs x_1
(Heat Source Velocity - Distributed Force)

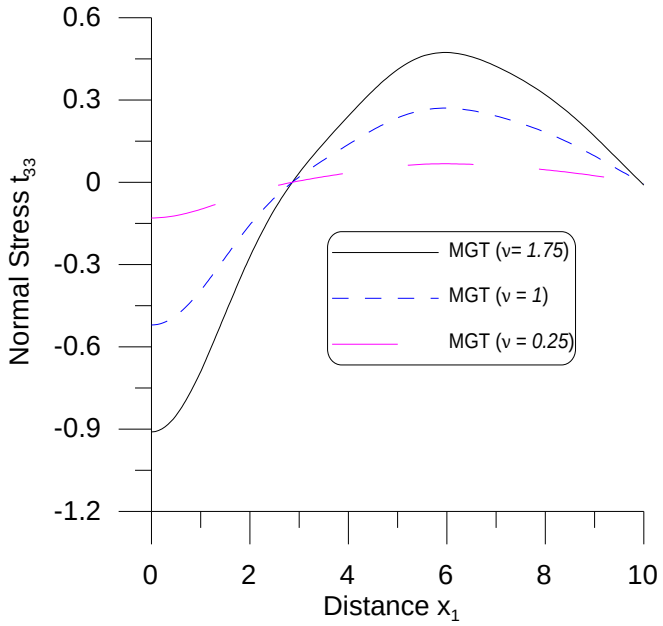

Fig. 13: Variation of t_{33} vs x_1
(Heat Source Velocity - Thermal Source)

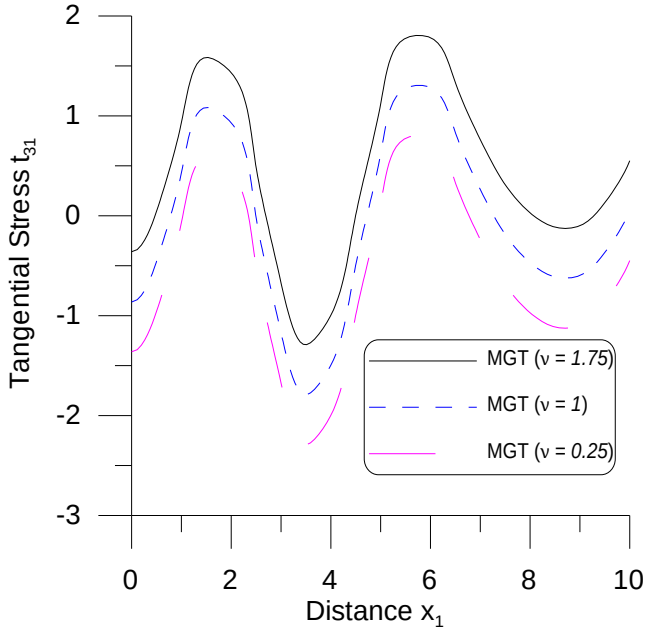

Fig. 14: Variation of t_{31} vs x_1
(Heat Source Velocity - Thermal Source)

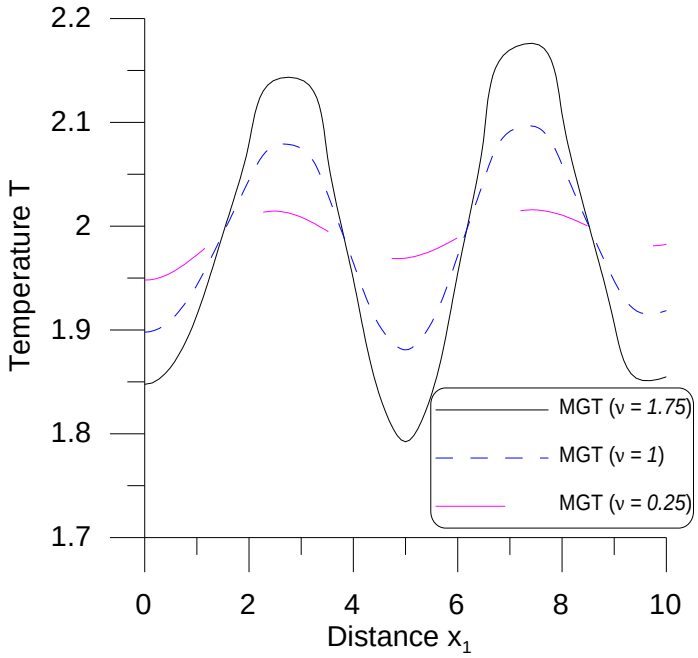

Fig. 15: Variation of T vs x_1
(Heat Source Velocity - Thermal Source)

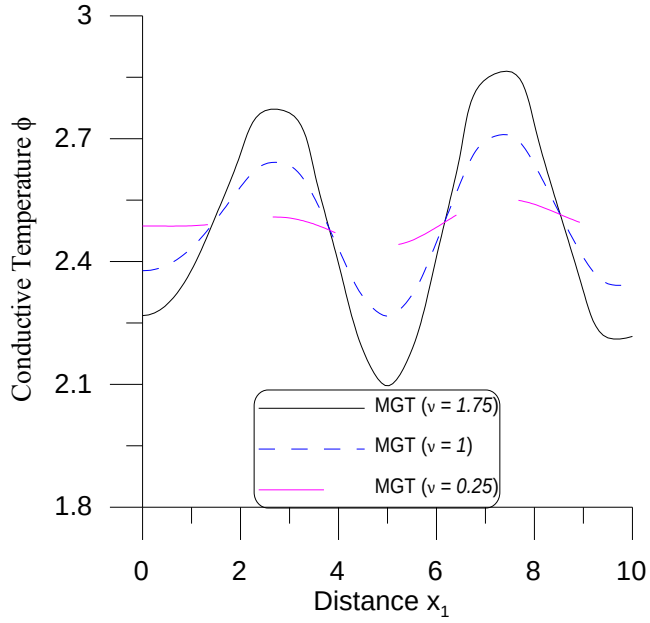

Fig. 16: Variation of ϕ vs x_1
(Heat Source Velocity - Thermal Source)

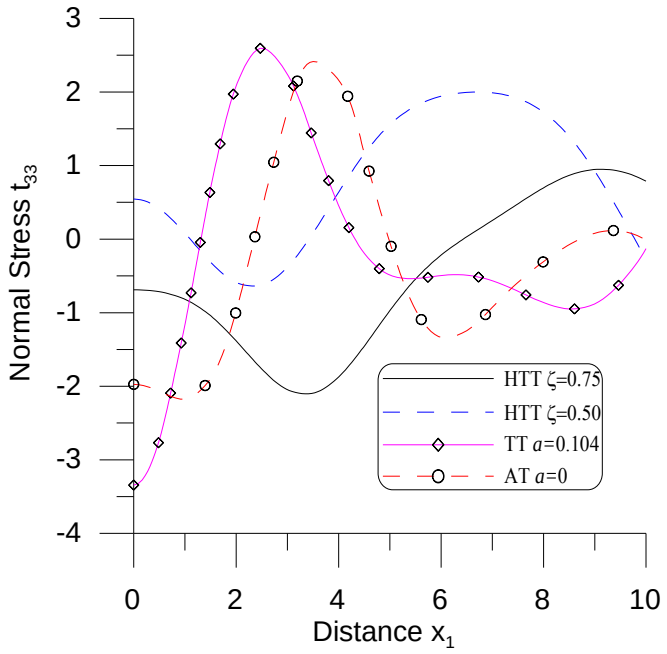

Fig. 17: Variation of t_{33} vs x_1
(Hyperbolic two temperature - Distributed Force)

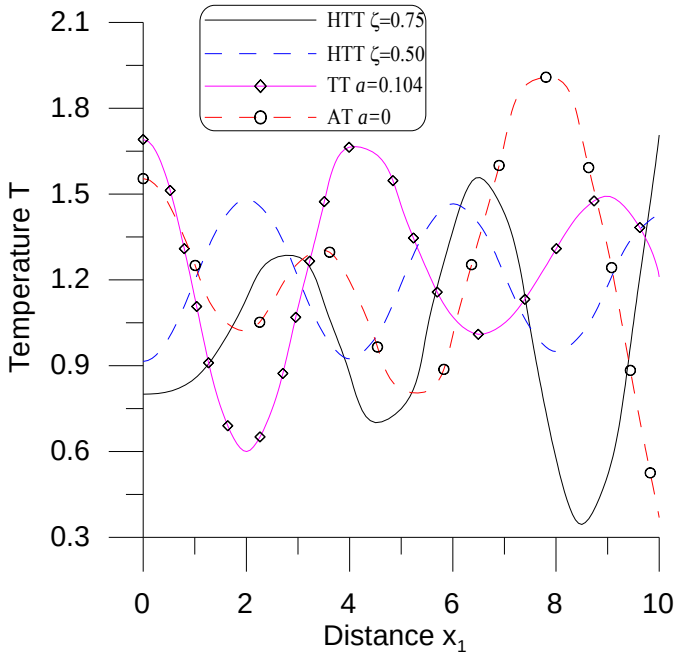

Fig. 19: Variation of T vs x_1
(Hyperbolic two temperature - Distributed Force)

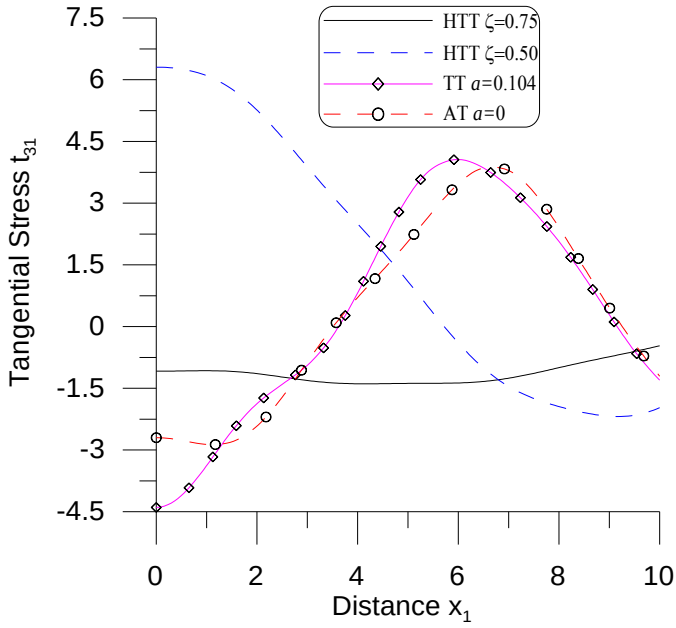

Fig. 18: Variation of t_{31} vs x_1
(Hyperbolic two temperature- Distributed Force)

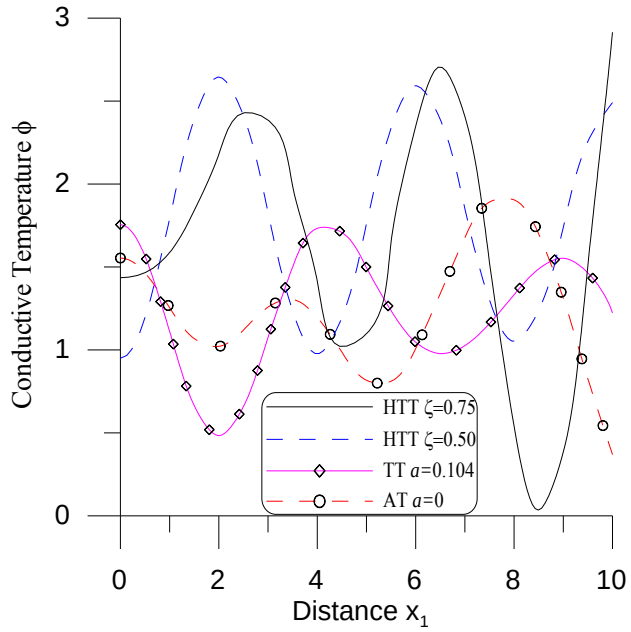

Fig. 20: Variation of ϕ vs x_1
(Hyperbolic two temperature - Distributed Force)

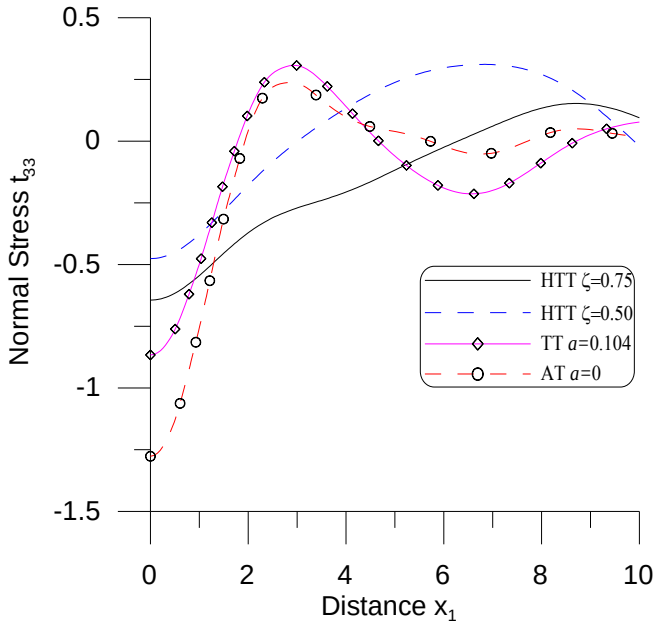

Fig. 21: Variation of t_{33} vs x_1
(Hyperbolic two temperature - Thermal Source)

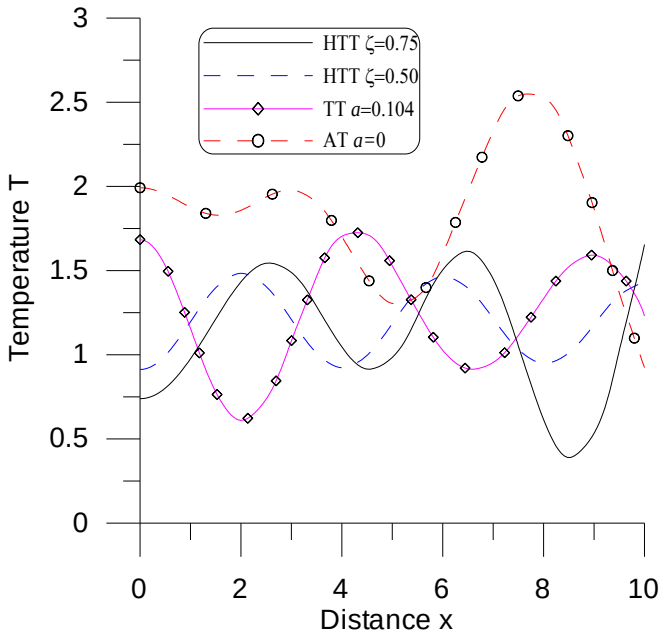

Fig. 23: Variation of T vs x_1
(Hyperbolic two temperature - Thermal Source)

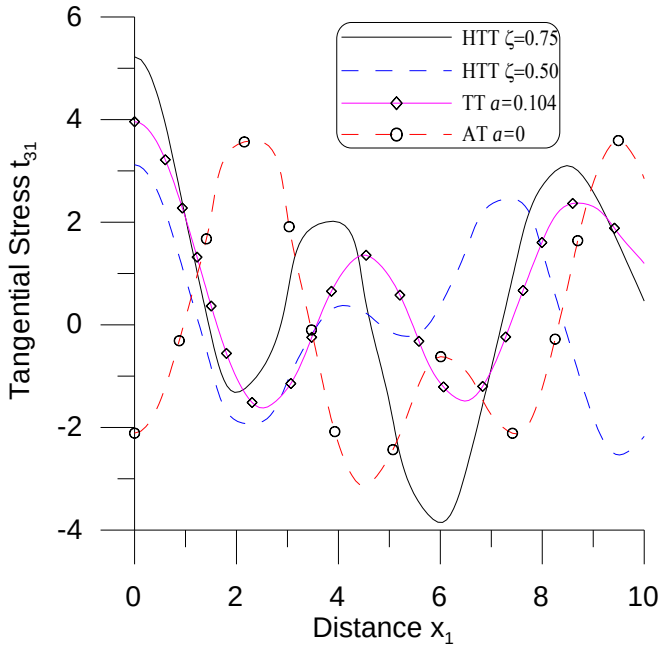

Fig. 22: Variation of t_{31} vs x_1
(Hyperbolic two temperature - Thermal Source)

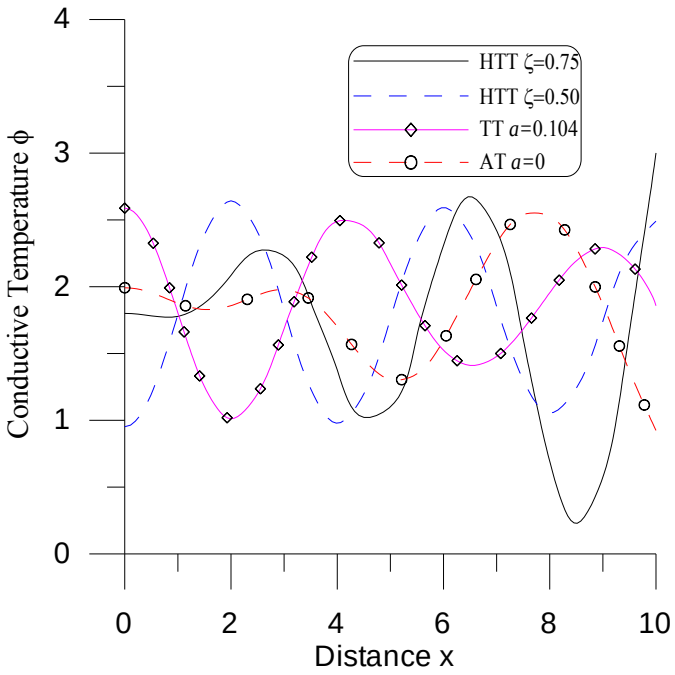

Fig. 24: Variation of ϕ vs x_1
(Hyperbolic two temperature - Thermal Source)